Classical Trajectory Study of Energy Transfer in Pyrazine−CO Collisions†

Cortney Higgins,‡ Quan Ju, Natalie Seiser, and George W. Flynn

Department of Chemistry, Columbia University, New York, New York 10027

Sally Chapman*

Department of Chemistry, Barnard College, New York, New York 10027-6598

Received: October 26, 2000; In Final Form: January 26, 2001

Classical trajectory calculations for collisions between vibrationally hot pyrazine ($E = 40332$ cm^{-1}) and room-temperature CO are compared with recent diode laser experiments. Ab initio calculations were carried out to determine parameters for the pairwise Lennard-Jones intermolecular potential. The trajectory results appear to show good qualitative agreement with preliminary experimental results. The highest ΔE collisions occur when the CO happens to lie above the pyrazine plane just as the underlying CH wag executes an unusually high amplitude motion. Artificially doubling the length of the CO produces results for the angular momentum transfer to the CO molecule that look quite similar to those for angular momentum transfer to CO_2 in analogous pyrazine−CO_2 experiments.

Introduction

Since the Lindemann mechanism was first proposed,[1] it has been understood that gas-phase unimolecular reaction rates depend not only on the intrinsic reaction rate of a decomposing reacting molecule but also on the associated rates of activation and deactivation: energy transfer among the colliding partners. Energy transfer has constituted a rich area of experimental and theoretical study.[2−4] Modem kinetic models, important in areas such as combustion and atmospheric chemistry, use master equations to describe rates of energy flow between reactive molecules and the surrounding bath. Accurate energy transfer rate constants and probability functions are essential to these models. Yet details about energy transfer are often not well-known. When the excitations involve larger molecules, aromatics like benzene and its derivatives, excited with chemically significant amounts of energy (∼100 kcal/mol), it is challenging both experimentally and theoretically to obtain detailed information.

A large body of experimental work on collisional energy transfer (CET) uses chemical methods of activation.[5] Laser-based physical methods can provide considerably greater detail, making more direct measurements of properties of the function that plays a central role in energy transfer, $P(E,E')$: the probability of energy transfer from E' to final energy E. Time-resolved infrared fluorescence (IRF) methods[6−9] have been applied to a number of large molecule systems. Single color IRF experiments give information about the energy dependence of the average energy transfer, $\langle \Delta E(E) \rangle$, the bulk-averaged first moment of $P(E,E')$. Of particular interest to this work, Miller and Barker[8] studied relaxation of excited pyrazine with 19 collision partners, including CO and CO_2. Two-color IRF studies provide more detailed information about the shape of the energy transfer function. This method has been applied to benzene−benzene[7] and pyrazine−pyrazine[9] CET. Time-resolved ultraviolet absorption (UVA) is a related technique, pioneered by Troe and co-workers.[10−13] Among the molecules studied are toluene,[10] azulene,[11] hexafluorobenzene,[12] and most recently, benzyl radicals,[13] colliding with various partners. Weisman and co-workers have studied energy loss from vibrationally excited triplet pyrazine by monitoring the energy dependent intersystem crossing rate from triplet to singlet.[14]

Kinetically controlled selective ionization (KCSI)[15−18] is a two-color pump−probe method that gives more detailed information about the function $P(E,E')$. Excellent agreement is obtained with experiment using a master equation analysis. In particular, this method gives accurate first and second moments of the distribution. Results have been presented for relaxation of azulene by collisions with *n*-heptane,[17] and of toluene with a variety of collision partners.[18] Interestingly, in the latter study, they find that a double exponential representation of $P(E,E')$ is required for smaller collision partners (He, Ar, and CO_2) while, for larger partners, a single-exponential function with parametric exponent gives a better fit.

In the methods above the relaxing hot molecule is observed. Experiments in our laboratory[19−26] use a different approach: a narrow diode laser is used to monitor the energy in the small (initially cold) collision partner, typically CO_2, under single collision conditions. Because the collision partner is small, fully state-resolved data are obtained. The diode laser line is sufficiently narrow that the Doppler profile of each final rotational line can be used to determine the post-collision translational energy. On the basis of these measurements, it is possible to extract[22] the exact shape of the high ΔE portion of the energy transfer function $P(E,E')$ under single collision conditions. This method has been used to study activated hexafluorobenzene,[22,23] pyrazine,[20−22,24,25] and methylpyrazine[26] with CO_2. In this paper, we describe preliminary results on vibrationally excited pyrazine colliding with a different cold bath gas, CO; a more complete experimental paper is in preparation.[27] Using similar teclmiques, Mullin and co-workers[28−32] have studied pyrazine/CO_2,[29,31] pyrazine/H_2O,[30]

† Part of the special issue "William H. Miller Festschrift".

* To whom correspondence should be sent.

‡ NSF REU summer undergraduate fellow at Columbia University, visiting from Hendrix College, Conway AR.

10.1021/jp003980i CCC: $20.00
Published on Web 03/03/2001

pyridine/CO_2,[28] and pyridine/H_2O.[32] They have paid particular attention to the dependence of the energy loss on the initial excitation energy.

In early models of CET, strongly deactivating collisions were assumed: collisions that result in substantial energy loss. Subsequent work demonstrated that most collisions are actually weak. Exponential energy loss functions became the norm.[5] But as experiments began to probe energy loss in greater detail, evidence appeared[14,15,33−35] for the existence of a small number of collisions that transfer significant amounts of energy: supercollisions. Even if the probability of supercollisions is small, their effect on average energy transfer is potentially large.[36] Thus, supercollision events continue to be of interest in collisional energy transfer.

The majority of theoretical studies of CET in aromatic systems have used classical trajectories. Many have probed relaxation of vibrationally excited (hot) polyatomics by collisions with a monatomic partner, although there have also been pioneering molecule- molecule studies. Gilbert and co-workers[37] studied relaxation of azulene with various rare gas partners. Lim studied toluene[38] energy transfer with both Ar and He. Bernshtein, Oref, and co-workers studied toluene[39] and benzene[40] with Ar. Lenzer et al.[41] studied benzene and hexafluorobenzene with He, Ar, and Xe. Of particular interest in this study was the importance of low-frequency modes to CET. Lenzer and Luther[42] studied benzene colliding with both He and Ar, with particular attention to the effects of different interaction potentials. Yoder and Barker[43] studied both predissociation of van der Waals cluster and CET in pyrazine and methylpyrazine with argon. In the first trajectory study of an excited aromatic colliding with a polyatomic bath gas, Lenzer and Luther studied benzene−benzene.[44] More recently[45] Grogoleit et al. have investigated in some detail the temperature dependence of energy transfer from azulene with several rare gas collision partners, along with pyrazine−pyrazine collisions.

Quantum mechanical treatment of dynamics involving molecules as large as these aromatics is immensely challenging; nevertheless, Clary and co-workers have made contributions in this area. Reduced-dimensionality quantum calculations showed quite good agreement with classical results in a study of benzene−rare gas[46] collisions; low-frequency out-of-plane modes were particularly important to the energy transfer. This confirms results of Lendvay and Schatz,[47] who compared classical and quantum mechanical results for relaxation of smaller excited molecules, particularly CS_2 colliding with various partners. Jordan and Clary[48] looked at energy transfer in electronically excited *p*-difluorobenzene. While this study included much less vibrational excitation of the polyatomic than in the present study, there was again quite satisfactory agreement between the quantum and classical results.

In this paper we report a classical trajectory study of vibrationally excited pyrazine colliding with the diatomic CO and compare with preliminary experimental results. In the experiments, pyrazine is excited with a 248 nm laser, and undergoes rapid radiationless decay to the ground electronic state. The vibrationally excited pyrazine molecules are quenched by collisions with thermal CO. A high-resolution CW infrared diode laser probes the nascent rovibrational states of CO. Rotational excitation is measured by looking at the transient absorption signal at the center of specific rotational lines. The transient absorption line profile can be measured with high accuracy under single collision conditions; this allows us to determine the translational recoil velocity, through the Doppler effect. In the calculations, we use the general classical trajectory program VENUS of Hase and co-workers,[49] with some modifications. We have replaced the Adams−Moulton integrator with a Hybrid Gear routine[50] that gives approximately an extra digit of energy conservation in a typical trajectory for the same integration step size. The calculations are done on Windows-based Dell PC's. A typical trajectory takes about 0.75 min on a 450 MHz Pentium III machine. Individual trajectories were animated using the VMD graphics package;[51] Hase[52] provided code to convert the trajectory output to suitable form.

TABLE 1: Pyrazine Vibrational Frequencies (cm^{-1})[a]

a	symmetry	Billes[b] calculation	VENUS	motion[c]
1	A_g	1003	1003	s-ring
2	A_g	3060	3041	s-CH
3	B_{3g}	1356	1356	b-CH/s-ring
6a	A_g	590	589	b-ring
6b	B_{3g}	673	673	b-ring
7b	B_{3g}	3041	3055	s-CH
8a	A_g	1585	1585	s-ring/b-CH
8b	B_{3g}	1528	1528	s-ring/b-CH
9a	A_g	1242	1241	b-CH/s-ring
12	B_{1u}	1011	1011	s-ring/b-ring
13	B_{1u}	3042	3041	s-CH
14	B_{2u}	1315	1314	s-ring
15	B_{2u}	1075	1075	s-ring/b-CH
18a	B_{1u}	1139	1139	s-ring/b-ring/b-CH
19a	B_{1u}	1486	1486	b-CH/s-ring
19b	B_{2u}	1425	1425	b-CH/s-ring
20b	B_{2u}	3055	3060	s-CH
4	B_{2g}	743	484	w-CH
5	B_{2g}	946	1250	t-ring
l0a	B_{1g}	941	1036	w-CH
11	B_{3u}	799	971	w-CH
16a	A_u	339	264	t-ring
16b	B_{3u}	420	393	t-ring
17a	A_u	958	1368	w-CH

[a] The last seven modes are out-of-plane. [b] Reference 53. [c] s = stretch, b = bend, t = torsion, w = wag.

Calculation Details

I. Potential Energy. *1. Pyrazine.* An experimental and theoretical study of pyrazine vibrations was recently published by Billes et al.[53] They obtained excellent agreement between frequencies derived from ab initio calculations and their experimental results. The full valence coordinate harmonic force field was kindly provided by Billes.[54] All of the parameters for the in-plane motions (bends and stretches), are easily incorporated in the data for the VENUS program. The 17 in-plane frequencies of the pyrazine are quite well represented in the model (Table 1).

At present, the VENUS program includes code for diagonal terms only for the out-of-plane motions (ring torsions and CH out of plane wags) so the full Billes force matrix could not be incorporated directly for these coordinates. Using PC-SPARTAN-PRO,[55] ab initio calculations (SCF with 6-31G* basis set and Moeller−Plesset second order perturbation) were carried out to study the out-of-plane CH wag motion, freezing all remaining atoms. Over a surprisingly large range of this wag coordinate α, the potential is quite well described by a harmonic function (Figure 1a). It takes about 100 kcal/mol to bend one CH to be perpendicular to the ring. The diagonal force constant $k_{\alpha\alpha}$ was determined from these data, and the two other diagonal constants (ring torsions) were varied to optimize the fit to the seven out-of-plane frequencies, with particular attention to the lowest frequency modes. The resulting agreement with experimental frequencies for these seven out-of-plane modes is not nearly as good as for the in-plane modes. (Table 1).

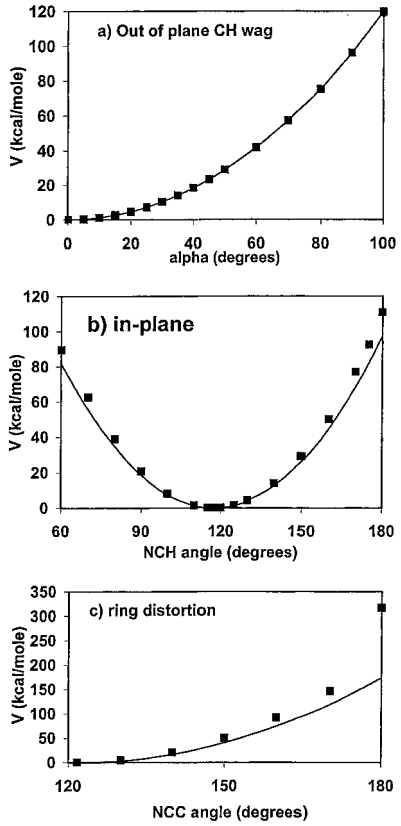

Figure 1. Results of ab initio calculations for selected deformations of pyrazine from its equilibrium geometry: (a) C−H out-of-plane wag; (b) C−H in-plane bend; (c) distortion of the ring. All distances are frozen while one angle is deformed. The other angles are minimized at the SCF level, and the energy of the corresponding structure is evaluated with MP2 correction. The solid line is the model potential evaluated at the same geometry with the parameters used in the dynamics calculation.

Pyrazine excited with a 248 nm laser has 40 322 cm^{-1} (115 kcal/mol) internal excitation. With excitations this large, one concern is that the trajectories will explore regions where the harmonic description of the potential might be seriously in error, or where the definitions of the valence coordinates are problematic. Several cases were explored with ab initio calculations: energies were calculated for distortions of pyrazine along a particular coordinate, and the resulting energies compared with harmonic functions. Figure 1b shows a single CH in-plane bending motion. A harmonic potential fits remarkably well, even for quite extensive displacements. It is also reassuring that it takes at least 100 kcal/mol to bring either an NCH or a CCH angle to 180°; if either angle were to become linear in a trajectory, there would be a discontinuity in the corresponding force. The probability that this much energy will be found in this one coordinate is very small. Figure 1c shows the in-plane distortion of an NCC angle toward 180°, with all bond lengths frozen and other angles relaxed. While the agreement between the model function and the ab initio results is not as good as for the CH bend, it is probably adequate. It was again reassuring that distorting an interior ring angle to 180° requires excitations on the order of 100 kcal/mol, since such a distortion would cause the definitions of the valence coordinates for both the ring torsion and the out-of-plane wag motion to fail.

In watching preliminary animations, we observed another problem with the initial pyrazine potential: in a test trajectory, one of the CH bonds flipped from the outside to the inside of the ring! Ab initio calculations show that it takes about 200 kcal/mol for this to happen. In VENUS, however, this out-of-plane wag angle α is defined in the interval −90° to +90°, so the continuing rise in energy as the H bends into the center of the ring (past 90°) is not correctly represented. These flips occurred rarely, since they require a large fraction of the energy in the excited pyrazine to concentrate in this one motion. To prevent this from happening, additional exponential terms were added between each H and the three atoms across the ring. Parameters were chosen so the CH out-of-plane deformation matched the Spartan calculations for $\alpha = 90$ and 100°; these were made quite steep so their contribution near the pyrazine equilibrium geometry is negligible.

Details and parameters for the pyrazine potential are available in the Supporting Information. The CO molecule is described by a Morse function with $D_e = 332.104$ kcal/mol, $r_e = 1.12832$ Å, and $\beta = 2.29898$ $Å^{-1}$.

2. Interaction Potential. The intermolecular potential was represented as a sum of pairwise terms, as is standard practice.[36−45] While this introduces a level of approximation, it is probably the only practical approach at this point for systems of this size. Lennard-Jones pair potentials are often used, with parameters determined using combining rules.[56] There have been some studies comparing various pair potentials. Lim[38] found that the steeper 12-6 potential produced greater energy transfer than an EXP-6 potential with the same well depth. Lenzer and Luther[42] observed that the details of the shape of the potential mattered more when the interaction well depth was small. They obtained best agreement with experiment using pair potentials derived from inelastic differential cross section data.

We chose to determine the parameters for the pairwise Lennard-Jones 12−6 terms using ab initio calculations. Since the pyrazine is colliding with a heternuclear diatomic molecule, we needed a way to determine and represent the anisotropy with respect to the CO of its interaction with pyrazine. The use of combining rules could very well have generated a potential of comparable (or better) quality; we present our approach as a reasonable alternate starting point.

Ab initio calculations (6-31G* MP2) were carried out for various approaches of CO to pyrazine, each at its equilibrium geometry, as determined by minimizing the geometry at the Hartree−Fock level, with the same basis. The resulting ∼250 points were used to find Lennard-Jones parameters for each of the six intermolecular atomic pairs (C−C, C−N, C−H and O−C, O−N, O−H). The least-squares fitting procedure included only those points whose interaction energy was below +2 milliHartrees (440 cm^{-1}) relative to separate molecules. This resulted in a reasonably good fit to the location and energies of the shallow wells corresponding to most directions of approach. Results are shown in Figure 2. The Lennard-Jones parameters are in Table 2. Note that for some of the pairs the C_6 coefficient is positive: these pairwise interactions are purely repulsive. The fit is better for approaches of CO normal to the pyrazine plane. The poorest fit is for in-plane approaches of CO along the axis between the two CH bonds: in the model the CO can slide between the atoms considerably farther than in the ab initio results.

However, other approaches toward H (in plane along the C−H axis or from above) are reasonably well described.

Several contour plots for slices of the surface are in Figure 3, showing approach of CO to a fixed pyrazine in various orientations. While there are several local minima, showing preferred approach normal to the ring or in-plane between the CH bonds, the ansiotropy is not great: a temporarily bound CO may move in various directions around the pyrazine molecule relatively easily.

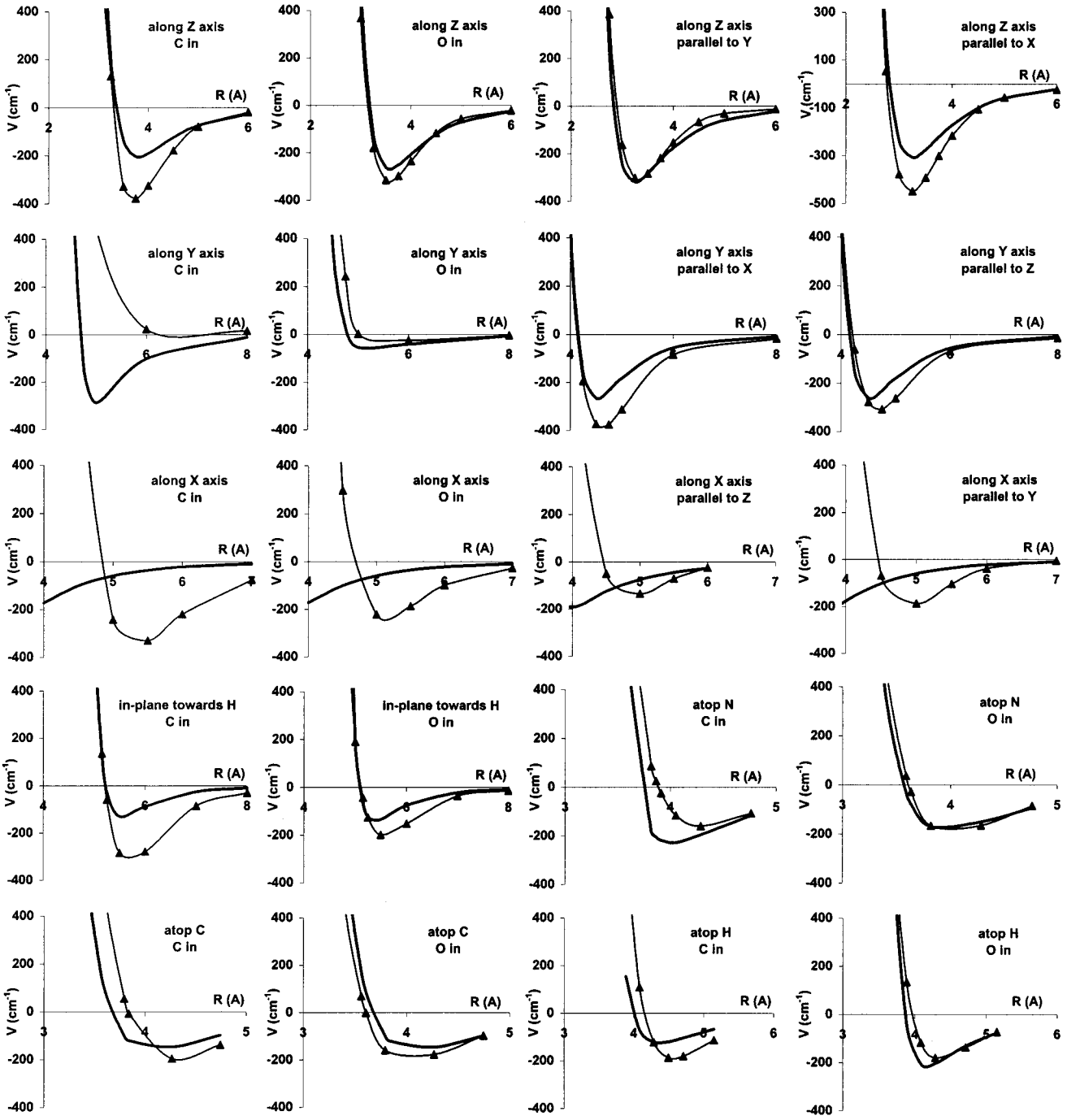

Figure 2. Ab initio calculation of intermolecular potential with least-squares fit to pairwise Lennard-Jones curves. The dark solid curves are the Lennard-Jones fit, the points (connected with light curves) are the ab initio results. Pyrazine is at the origin of the Cartesian frame, lying in the *XY* plane with the *Y*-axis passing through the nitrogen atoms. CO approaches along various axes, with various CO orientations. The first three rows show approach along the Cartesian axes: row 1, along *Z* (normal to pyrazine plane); row 2, along *Y* (approaching an N atom); row 3, along *X* (between the CH bonds). In the first column the CO is oriented with the C atom in, in the second column O is in, and in the last two columns CO is perpendicular to the direction of approach. The first two frames of row four show an additional in-plane approach, along a line passing from the origin through one H atom. The remaining frames show approaches along lines normal to the pyrazine plane: row 4, above N, and row 5, above C and above H.

This intermolecular potential is approximate at best. The ab initio points were calculated with the two molecules at their equilibrium geometries only. Moreover, the quality of the fit to the calculated points is not high. The fact that some of the pairwise terms have wells (attractive r^{-6} terms) while others do not, is curious. We do not claim that properties such as the location and depths of the various minima are well represented. As is always true, the best test of the potential is in the dynamics.

II. Dynamics. Options in the VENUS trajectory program were used to define the trajectory initial conditions. The CO begins in a specific quasiclassical (v, J) state. A vibrational energy is specified for pyrazine, along with its rotational temperature. The relative translational energy is selected from a thermal distribution at a specified temperature. Some 50 initial and final parameters are stored for each trajectory; results from multiple batches may then be combined and analyzed separately. All reported trajectory average quantities have been normalized so they are reported per Lennard-Jones collision:[57] multiplied by $[b_{max}^2/(\Omega(2,2)\ b_{LJ}^2)]$, where $\Omega(2,2)$ is the Lennard-Jones collision integral and b_{LJ} is the Lennard-Jones impact parameter.

TABLE 2: Lennard-Jones Parameters: $V = C_{12}/r^{12} - C_6/r^6$ (When $C_6 > 0$ Position and Depth of the Attractive Well Are Included)

atom pair	C_{12} [(kcal Å^{12})/mol]	C_6 [(kcal Å^6)/mol]	r_e (Å)	ϵ (cm^{-1})
C−N	926951.62	2296.48	2.7185	1989.91
C−C	1688835.70	−301.53		
C−H	18977.589	187.25	2.1593	646.20
O−N	229549.81	−513.90		
O−C	347193.88	682.41	2.8255	469.12
O−H	35461.04	173.17	2.4278	295.77

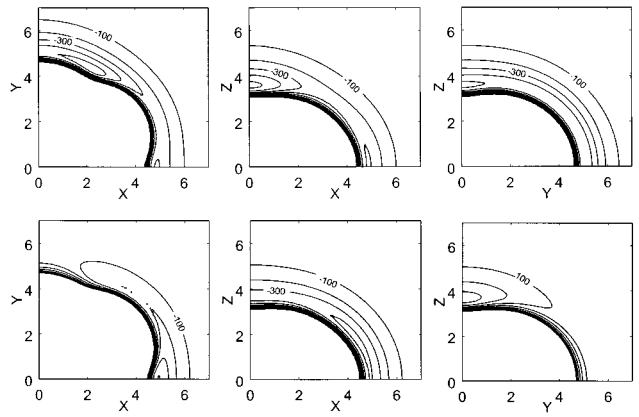

Figure 3. Contour plots of the intermolecular potential between pyrazine and CO. Pyrazine is at the origin of the Cartesian frame, lying in the *XY* plane, with the *Y*-axis passing through the nitrogen atoms. The CO molecule lies in the *XY*, *XZ*, and *YZ* planes. The CO bond points toward the origin. In the upper frames the C atom points in, while in the lower the O atom points in. Distances are in angstroms measured from the center of the pyrazine to the midpoint of the CO. Equipotential contour curves are shown in intervals of 100 cm^{-1}, with the highest contour at +500 cm^{-1}.

The value used for b_{LJ}, 4.525 Å, is half the sum of Lennard-Jones diameters, d_{CO}, 3.70 Å,[58] and $d_{pyrazine}$, assumed to be that of benzene, 5.35 Å,[58] as in refs 8 and 20.

Choosing a maximum impact parameter can be challenging when studying energy transfer collisions. In principle, one wants a large enough value so that all collisions at larger *b* make no contribution to the properties of interest. Most collisions at very large impact parameters are essentially elastic. However, even at very large impact parameters, a very small fraction of collisions, typically those with little initial relative velocity, drawn by the long-rarige attractive force, spiral in to experience a close collision. For a sample set of initial conditions, we ran 10 000 trajectories with a b_{max} of 9 Å. These were then supplemented with another batch of 1664 with *b* between 9 and 9.72 Å. A few close collisions occur in the supplementary batch: 16 lead to nonzero changes in the histogrammed final *J* state of CO, but average quantities were the same to 0.1%. A maximum impact parameter of 9 Å was used for subsequent calculations.

Results and Discussion

In this preliminary study, the trajectories simulate one set of conditions examined in the laboratory. Pyrazine has vibrational energy corresponding to 248 nm excitation plus zero-point energy (56 700 cm^{-1} total). The temperature is 300 K, for both translation and pyrazine rotation. CO is given quasiclassical excitation corresponding to $v = 0$, $J = 10$. (The experiments have a thermal distribution of CO rotational states; $J = 10$ is near the average.) A total of 10 000 trajectories were included. Collision with hot pyrazine has negligible effect on CO vibration: the average change in the vibrational action parameter (the classical equivalent of the vibrational quantum number) is +0.001 with rms value 0.051; only one out of 10 000 trajectories has a change in action greater than 0.5, which would be characterized as vibrational excitation, using simple histogram methods. Although the data have not yet been fully analyzed, the experiments too indicate little vibrational excitation.

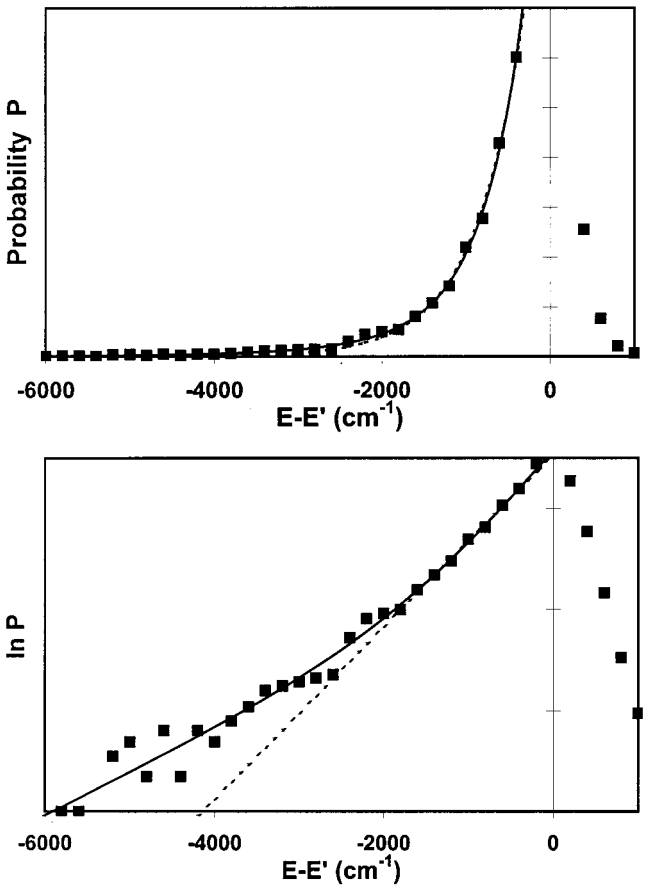

Figure 4. Energy transfer probability $P(E,E')$. Trajectory results are collected in bins 200 cm^{-1} wide. The elastic peak (interval from −100 to +100 cm^{-1}) is off scale. Since the shape is the main object of interest, the function has not been normalized; hence no scale is given on the ordinate. The solid line is a least-squares fit of the downward ($\Delta E < 0$) transitions to a double exponential with widths $\alpha_1 = -497$ cm^{-1} and $\alpha_2 = -1168$ cm^{-1}, the dotted line is a fit to a single exponential ($\alpha = -586$ cm^{-1}). The first inelastic point (bin centered at $\Delta E = -200$ cm^{-1}) was excluded from the fit. The logarithmic plot provides evidence of the inadequacy of a single-exponential fit.

On average, pyrazine loses 502 cm^{-1} internal energy per Lennard-Jones collision; 183 cm^{-1} goes into CO rotation and 324 cm^{-1} into translation. The average change in *J* for CO is 1.9, with the largest observed final $J = 48$. Rotation increases in pyrazine too: the average length of the angular momentum vector, initially 41.4$\hbar$, changes by 12.2$\hbar$. Rotation and vibration are strongly coupled in this highly excited molecule, so separate energies for pyrazine vibration and rotation are not reported.

The calculated pyrazine energy transfer function $P(E,E')$ is shown in Figure 4. The average energy gain for the upward collisions is 206 cm^{-1}, while the average energy loss in downward collisions is 956 cm^{-1}. Pyrazine loses energy in 59% of the trajectories. The downward transitions were fit with a double-exponential function:

$$P = A\{(1 - f)\exp(-\Delta E/\alpha_1) + f\exp(-\Delta E/\alpha_2)\}$$

with $\alpha_1 = 479$ cm^{-1}, $\alpha_2 = 1168$ cm^{-1}, and $f = 0.12$. These

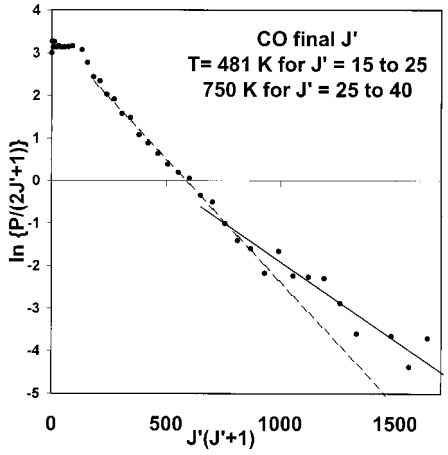

Figure 5. Rotation of CO after single collision, fit to a thermal distribution. The plot is linear for limited ranges of final *J*. Least-squares fitting of points between $J = 12$ and 25 gives a temperature of 481 ± 17 K, whereas between 25 and 40, the temperature is 750 ± 56 K (uncertainties represent one standard deviation in the least-squares fit).

values, however, must be taken as quite approximate, since they are somewhat sensitive to the choice of histogram bin size and how many bins adjacent to the elastic peak are excluded from the fit. Thus, better statistics is needed for a precise representation of the large ΔE tail of $P(E,E')$. The above numbers are for a bin size of 200 cm^{-1}, omitting the first inelastic interval ($\Delta E = -200$ cm^{-1}) from the fit. A single exponential fit [$P = A_0 \exp(-\Delta E/\alpha)$] with $\alpha = 586$ cm^{-1} is shown for comparison; it fails to account for the high ΔE events.

The analysis determining the average energy transfer from our diode laser experiments is not yet complete, so we can make no direct comparison between calculated and experimental $\langle \Delta E \rangle$ values at this excitation energy. Miller and Barker[9] measured pyrazine/CO relaxation, with an initial excitation of 32 500 cm^{-1}. From this IRF experiment, they obtained a polynomial fit for $\langle \Delta E \rangle_{down}$ and $\alpha(E)$. Extrapolated to our excitation energy, their results give $\langle \Delta E \rangle_{down} = 199$ cm^{-1} and $\alpha = 145$ cm^{-1}, both significantly less than our trajectory results. While KCSI experiments[18] often give larger ΔE's than IRF or UVA experiments, particularly at higher excitation energies, it is quite likely that our calculated average energy transfers are too large.

The CO molecule begins in a fixed *J* state: a microcanonical distribution. There is no reason to expect that a thermal (canonical) distribution will be established after a single collision. However, since a broad range of final J' states is observed, it is useful to analyze the final CO *J* state distribution in terms of a thermal distribution, as shown in Figure 5. Since all trajectories start with $J = 10$, the $J' = 10$ peak includes a large elastic component. No single temperature describes the distribution for small ΔJ. There is, however, linear behavior, suggestive of a rotational temperature, for the larger ΔJ transitions. While the statistical uncertainty is significant, there is the appearance of two temperatures. Least-squares fitting of the states between $J = 15$ and 25 give a *T* of 481 ± 16 K, while those between $J = 25$ and 40 give a *T* of 750 ± 56 K, where the uncertainties represent one standard deviation in the least-squares fit. The latter is in reasonable agreement with preliminary experimental results, which indicate a final rotational temperature of 950 K for CO *J* states between 20 and 36.

A further comparison with experiment is in the rotational state dependence of the recoil velocity. The root-mean-square relative velocities were calculated for each final rotational state of CO; results are shown in Figure 6. Error bars represent the usual $1/N^{1/2}$ Monte Carlo relative uncertainty. While the small number

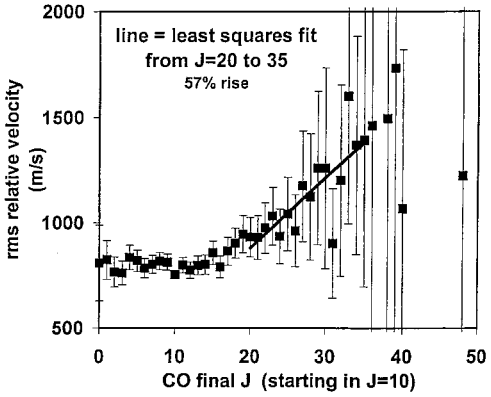

Figure 6. Correlation of final relative velocity with rotational state of the CO. The root-mean-square velocity is shown as a function of final *J*; error bars represent the statistical uncertainty associated with.the sampling. There is evidence for an increase in speed with *J*, particularly for the higher *J* collisions. The velocity increases 57% between $J = 20$ and $J = 35$ (as determined by least squares). This increase is comparable to that determined from the experimental Doppler profiles of the rotational lines for CO.

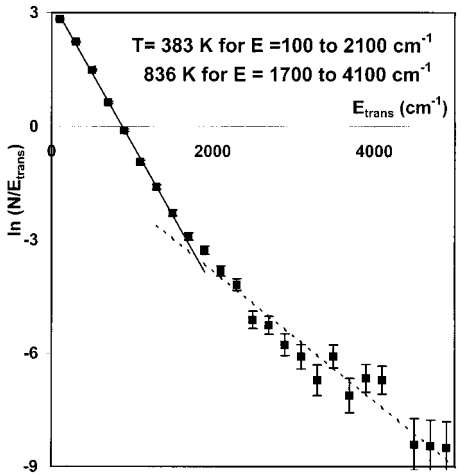

Figure 7. Determination of the average translational temperature after one collision. Trajectory results for all CO final *J* states have been collected in 200 cm^{-1} intervals. The logarithm of the number of trajectories per bin divided by its mean translational energy is shown as a function of translational energy. Since the initial translational energy is sampled from a thermal distribution, quasi-elastic large impact parameter collisions make a significant contribution at lower final translational energies. The higher energy tail of the distribution (to which elastic events do not contribute) suggests a translational temperature about 836 K. Error bars represent one standard deviation resulting from the statistical sampling.

of events make the larger ΔJ results quite uncertain, the increase in velocity as *J* increases is quite convincing. This linear increase is consistent with the experiments, where the observed recoiling CO Doppler width increases linearly with *J*; the magnitudes of the increase are comparable: the calculated velocities increase 56% and the experimental Doppler widths increase 66% between $J = 20$ and $J = 35$.

The final translational energy distribution, averaged over all *J*'s, is analyzed in Figure 7. The lower energy portion, fit to a thermal distribution, is reasonably linear with temperature 383 ± 6 K. However, there is a sizable contribution in this region from quasi-elastic large impact parameter collisions. The higher energy tail is characterized by a higher temperature; fitting between 1700 and 4100 cm^{-1} gives a translational temperature of 836 ± 82 K (above 4100 cm^{-1} there is no more than one trajectory per bin).

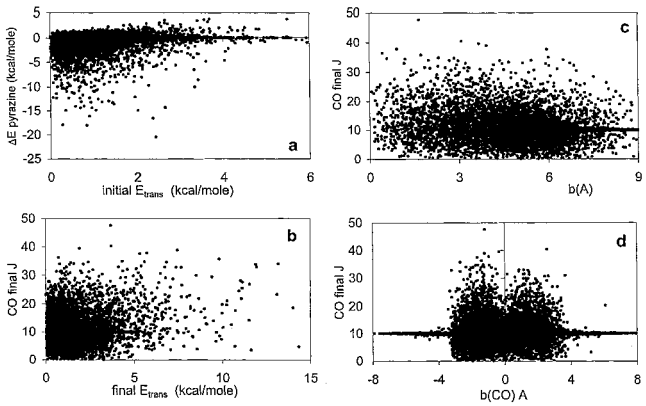

Figure 8. Scatter plots showing correlations among selected collision parameters. Each point represents a collision. In some cases, a dark horizontal line results from large impact parameter quasi-elastic collisions. (a) Pyrazine internal energy loss as a function of the initial relative translational energy (three points at higher translational energies are not shown). (b) Final rotational state of CO as a function of final translational energy; (three points at higher translational energies are not shown). (c) Final rotational state of CO as a function of the impact parameter. (d) Final rotational state of CO as a function of an impact parameter defined in Figure 9.

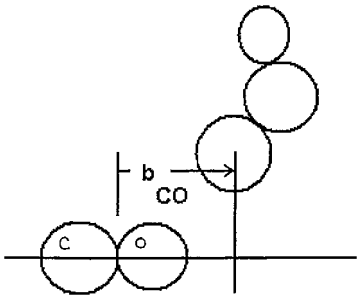

Figure 9. Definition of impact parameter on the CO (bco): the distance from the center of mass of the CO to a point along its axis intersected by a perpendicular dropped from the center of the nearest atom in pyrazine at the time of the first zero in the relative velocity (the first turning point).

As in previous trajectory studies on aromatic systems,[39−41,46] high ΔE collisions are present: $P(E,E')$ has an apparent large ΔE tail, and a small number of collisions produce very large CO(J); the largest J seen in this batch was 48. Is there a distinct mechanism for these events? Trajectories may be monitored for a variety of properties. The number of turning points in the relative velocity distinguishes a direct encounter from a short (or even long) lived complex. On the basis of a comparison of the $\Delta E = 0$ peak of the $P(E,E')$ curve with the exponential fit, about 45% of these trajectories are essentially elastic events. Of the inelastic collisions, about 72% were direct, 15% separated after a second bounce, 6% after three; the remaining 7% were quite complex: one bounced 14 times before separation, while one (of 10 000) was incomplete due to an upper time limit imposed on the trajectories. But large ΔE_{pyr} and ΔJ_{CO} events occurred for both direct and complex collisions.

Figure 8 shows four correlations among trajectory parameters. Panel a shows the pyrazine internal energy transfer as a function of the initial translational energy. It is clear that translational energy correlates with energy *gain* in the pyrazine, but large energy loss occurs for both fast and slow collisions. Panel b correlates two product properties: CO rotation with product translation energy. As discussed above, on average translational energy increases with J for higher final J. However, this average behavior masks broad distributions: large J's occur with both large and small translational energies, and large translational energies occur with both large and small ΔJ's. Panel c shows the CO product rotational state as a function of the traditional impact parameter. The quasi-elastic contribution can be seen in the dark horizontal band at $J = 10$. As was discussed above, some large b events still produce sizable ΔJ. More than 2000 trajectories are in the interval between 8 and 9 Å, so the 10 or so decidedly inelastic events are a small fraction. Small impact parameter events, head-on collisions, give rise to larger energy transfers, but the very large ΔJ collisions occur at a wide range of b's. Panel d correlates CO rotation with a different impact parameter, defined as the perpendicular distance along the CO axis (measured from the center of mass, with C on the negative and O in the positive axis) of the nearest atom in pyrazine at the moment of the first turning point in the relative velocity (see Figure 9). The sharp edge of the CO molecule, especially at the C end, is clear. Largest ΔJ events correlate with off-center collisions.

Viewing trajectory animations is a seductive and entertaining activity. The risk is that patterns will be inferred from what is a very small and not representative sample. However, with very large systems and complicated trajectories, such animations may provide useful insight. We looked at many animations, focusing especially on collisions that resulted in large energy transfer. Obvious in the animations was the expected chaotic motion of the pyrazine, with rapid and irregular energy flow within the molecule. In particular, CH bonds often have rather small amplitude in out-of-plane wag motion, but on occasion these wags are extreme. Such large amplitude wags play an important role in rotational excitation of the CO: in most collisions producing very large CO rotation, the CO moved into a position above the pyrazine plane at just the right moment to experience a swift kick, sending it tumbling away. This occurs both in direct (one turning point) and in complex collisions, after the CO has spent some time wandering around, trapped in the attractive potential. The orientation of the CO at the point of the kick is clearly important: if the impact hits CO on the side, nearly midway, large translational energy is produced. If the impact hits CO on the side, toward one or the other end of the molecule, large rotational energy is produced.

These observations are consistent with previous work. Bernshtein and Oref observed[40] that large ΔE events resulted from collisions in which the bath molecule lies perpendicular to a wagging C−H bond; the new factor here is that this can produce internal as well as translational energy in the bath. Moreover, the importance of low-frequency modes to energy transfer is well-established.[41,47,48] Large ΔE collisions are commonly observed in trajectory calculations;[39−41] indeed there is evidence that trajectories seriously overestimate their importance.[18] Our results are consistent with the emerging consensus that super-collisions do not constitute a distinct category of collisions but instead are rare events in the long tail of the function $P(E,E')$ whose shape is often not a simple single exponential.

"Long CO". The current pyrazine−CO experiments complement earlier ones with CO_2 as bath molecule.[20−22,24,25] While correct modeling of CO_2 would require a new intermolecular potential and detailed treatment of the triatomic, including its multiple vibrational modes, in a very simple picture, one could view this linear CO_2 molecule as a longer version of CO. To see what such a model would show, we compared the above results with some in which the length of the CO molecule was artificially doubled, without changing any other potential parameters. Results are shown in Table 3. The longer rotor does not produce major changes in the average energies transferred. Comparing $J = 10$ for normal CO with $J = 20$ for long CO,

TABLE 3: Doubling the Length of the CO Acceptor: Comparison of Average Values per LJ Collision

quantity	normal CO ($J = 10$)	long CO ($J = 10$)	long CO ($J = 20$)
$\langle E - E' \rangle$ (cm^{-1})	−502	−587	−563
$\langle E - E' \rangle_{up}$ (cm^{-1})	212	181	218
$\langle E - E' \rangle_{down}$ (cm^{-1})	−985	−992	−1051
% down	57.8	65.5	61.6
$\langle \Delta J \rangle_{pyr}$	12.2	7.7	11.2
$\langle \Delta E_{trans} \rangle$ (cm^{-1})	324	212	327
$\langle \Delta E_{rot} \rangle_{CO}$ (cm^{-1})	183	334	233
$\langle \Delta J \rangle_{CO}$	1.9	14.5	5.1
largest CO final J	48	88	111

the average change in the rotational energy of the CO is not very different; but this, of course, means that the population of high final J states in the final CO is strongly enhanced: the average value of ΔJ has increased by more than a factor of 2. The distribution of final J states for the long CO are quite comparable to those observed experimentally for pyrazine−CO_2 V → R,T collisions,[20] although averages over a distribution of initial J states must be made before a quantitative comparison can be made. However, these results are suggestive that a determining factor in the differences between CO and CO_2, at least for the V → R,T events, is the length of the rotor.

Conclusion

Classical trajectory calculations for collisions between vibrationally hot pyrazine and cold collision partner CO appear to show qualitative agreement with preliminary experimental results. After a single collision with hot pyrazine, there is little vibrational excitation of the CO. The CO molecules have a distribution of rotational states that can, at least for the higher J states, be described by a rotational temperature around 700 K. Recoil velocities increase with the final CO rotational state for the higher CO J levels. There is evidence for a biexponential $P(E,E')$, although the statistics for large ΔE events make the determination of the parameters uncertain. The very high AE collisions (supercollisions) occur when the CO sits above the pyrazine plane just as the underlying CH wag executes an unusually high amplitude motion. On the other hand, the calculated average energy transfer is too large, significantly larger than that extrapolated from the results of Miller and Barker.[8] While this may suggest that our intermolecular potential is somewhat flawed, the qualitative features of the model are likely to be correct. This study has focused on a single pyrazine excitation, one temperature for translation and pyrazine rotation, and a single CO initial rotational state. The effects of varying these parameters, as well as looking at different mass combinations, will be the focus of a future publication.

Acknowledgment. We thank Prof. Bill Hase for providing us a copy of the VENUS program and for some useful discussions. This work was supported by the Department of Energy under grant DE-FG02- 88ER13937. Equipment support was provided by the National Science Foundation under grantCHE-97-27205. Support for C.H. was provided under NSF's R.E.U. grant to the Columbia Chemistry Department, CHE-95-31382.

Supporting Information Available: The parameters for the pyrazine intramolecular potential. This material is available free of charge via the Internet at http://pubs.acs.org.

References and Notes

(1) Lindemann, F. A. *Trans. Faraday Soc.* **1922**, *17*, 598.
(2) Oref, I.; Tardy, D. C. *Chem. Rev.* **1990**, *90*, 1407.
(3) Weston, Ralph, E., Jr.; Flynn, G. W. *Annu. Rev. Phys. Chem.* **1992**, *43*, 559.
(4) Flynn, G. W.; Parmenter, C. S.; Wodtke, A. M. *J. Phys. Chem.* **1996**, *100*, 12817.
(5) Baer, T.; Hase, W. L. *Unimolecular Reaction Dynamics, Theory and Experiment;* Oxford University Press: New York, 1996.
(6) Barker, J. R.; Toselli, B. M. *Int. Rev. Phys. Chem.* **1993**, *12*, 305. Barker, J. R.; Brenner, J. D.; Toselli, B. M. *Adv. Chem. Kinet. Dynam.* **1995**, *2B*, 393.
(7) Brenner, J. D.; Erinjeri, J. P.; Barker, J. R. *Chem Phys* **1993**, *175*, 99.
(8) Miller, L. A.; Barker, J. R. *J. Chem. Phys.* **1996**, *105*, 1383.
(9) Miller, L. A.; Cook, C. D.; Barker, J. R. J. *Chem. Phys.* **1996**, *105*, 3012.
(10) Hippler, H.; Troe, J.; Wendelken, H. J. *J. Chem. Phys.* **1983**, *78*, 6709. Hippler, H.; Troe, J.; Wendelken. H. J. *J. Chem. Phys.* **1983**, *78*, 6718.
(11) Darnmm, M.; Hippier, H.; Troe, J. *J. Chem. Phys.* **1988**, *88*, 3564. Damm, M.; Deckert, F.; Hippler, H.; Troe, J. *J. Phys. Chem.* **1991**, *95*, 2005.
(12) Damm, M.; Hippler, H.; Olschewski, H. A.; Troe, J.; Willner, J. *Z. Phys. Chem.* **1990**, *166*, 129.
(13) Damm, M.; Deckert, F.; Hippler, H. *Ber. Bunsen-Ges.* **1997**, *101*, 1901.
(14) Bevilacqua, T. J.; Andrews, B. K.; Stout, J. E.; Weisman, R. B. *J. Chem. Phys.* **1990** *92*, 4627. Bevilacqua, T. J.; Weisman, R. B. *J. Chem. Phys.* **1993**, *98*, 6316. McDowell, D. R.; Wu, F.; Weisman, R. B. J. *Phys. Chem. A* **1997**, *101*, 5218.
(15) Luther, K.; Reihs, K. *Ber. Bunsen-Ges. Phys. Chem.* **1988**, *92*, 442.
(16) Hold, U.; Lenzer, T.; Luther, K.; Reihs, K.; Symonds, A. C. *Ber. Bunsen-Ges.* **1997**, *101*, 552.
(17) Hold, U.; Lenzer, T.; Luther, K.; Reihs, K.; Symonds, A. C. *J. Chem. Phys.* **2000**, *112*, 4076.
(18) Lenzer, T.; Luther, K.; Reihs, K.; Symonds, A. C. *J. Chem. Phys.* **2000**, *112*, 4090.
(19) Mullin, A. S.; Park, J.; Chou, J. Z.; Flynn, G. W.; Weston, R. E., Jr. *Chem. Phys.* **1993**, *175*, 53.
(20) Mullin, A. S.; Michaels, C. A.; Flynn, G. W. *J. Chem. Phys.* **1995**, *102*, 6032.
(21) Michaels, C. A.; Mullin, A. S.; Flynn, G. W. *J. Chem. Phys.* **1995**, *102*, 6682.
(22) Michaels, C. A.; Flynn, G. W. *J. Chem. Phys.* **1997**, *106*, 3558.
(23) Michaels, C. A.; Lin, Z.; Mullin, A. S.; Tapalian, H. C.; Flynn, G. W. *J. Chem. Phys.* **1997**, *106*, 7055.
(24) Michaels, C. A.; Mullin, A. S.; Park, J.; Chou, J. Z.; Flynn, G. W. *J. Chem. Phys.* **1998**, *108*, 2744.
(25) Sevy, E. T.; Muyskens, M. A.; Rubin, S. M.; Flynn, G. W.; Muckerman, J. T. *J. Chem. Phys.* **2000**, *112*, 5829. Sevy, E. T.; Muyskens; M. A.; Rubin, S. M.; Flynn, G. W. *J. Chem. Phys.* **2000**, *112*, 5844.
(26) Sevy, E. T.; Rubin, S. M.; Lin, Z.; Flynn, G. W. *J. Chem. Phys.* **2000**, *113*, 5844.
(27) Seiser, N.; Ju, Q.; Flynn, G. W. Manuscript in preparation.
(28) Wall, M. C.; Stewart, B. A.; Mullin, A. S. *J. Chem. Phys.* **1998**, *108*, 6185.
(29) Wall, M. C.; Mullin, A. S. *J. Chem. Phys.* **1998**, *108*, 9658. Wall, M. C.; Lemoff, A. S.; Mullin, A. S. *J. Phys. Chem. A* **1998**, *102*, 9101. Wall, M. C.; Lemoff, A. S.; Mullin, A. S. *J. Chem. Phys.* **1999**, *111*, 7373.
(30) Fraelich, M.; Elioff, M. S.; Mullin, A. S. *J. Phys. Chem. A* **1998**, *102*, 9761.
(31) Elioff, M. S.; Wall, M. C.; Lemoff, A. S.; Mullin, A. S. *J. Chem. Phys.* **1999**, *110*, 5578.
(32) Elioff, M. S.; Fraelich, M.; Sansom, R. L.; Mullin, A. S. *J. Chem. Phys.* **1999**, *111*, 3517.
(33) Lohmannnsroben, H.; Luther, K. *Chem. Phys. Lett.* **1988**, *144*, 473.
(34) Pashutzky, A.; Oref, I. *J. Phys. Chem.* **1980**, *92*, 178.
(35) Hassoon, S.; Oref, I.; Steel, C. *J. Chem. Phys. 1988*, *89*, 1743. Morgulis, I. M.; Sapers, S. S.; Steel, C.; Oref, I. *J. Chem. Phys.* **1989**, *90*, 923.
(36) Bernshtein, V.; Oref, I. *J. Phys. Chem.* **1993**, *97*, 12811. Bernshtein, V.; Oref, I. *J. Phys. Chem.* **1994**, *98*, 3782. Bernshtein, V.; Oref, I.; Lendvay, G. *J. Phys. Chem. A* **1997**, *101*, 2445.
(37) Lim, K. F.; Gilbert, R. G. *J. Phys. Chem.* **1990**, *94*, 77. Clarke, D. L.; Oref, I.; Gilbert, R. G.; Lim, K. F. *J. Chem. Phys.* **1992**, *96*, 5983. Clarke, D. L.; Gilbert, R. G. *J. Phys. Chem.* **1992**, *96*, 8450.
(38) Lim, K. F. *J. Chem. Phys.* **1994**, *100*, 7385. Lim, K. F. *J. Chem. Phys.* **1994**, *101*, 8756.
(39) Bernshtein, V.; Oref, I. *Chem. Phys. Lett.* **1995**, *233*, 173. Bemshtein, V.; Oref, I. *J. Chem. Phys.* **1996**, *104*, 1958. Bernshtein, V.; Lim, K. F.; Oref, I. *J. Phys. Chem.* **1995**, *99*, 4531.

(40) Bernshtein, V.; Oref, I. *ACS Symp. Ser.* **1997**, *678*, 251. Bemshtein, V.; Oref, I. *J. Chem. Phys.* **1997**, *106*, 7080. Bemshtein, V.; Oref, I. *Chem. Phys. Lett.* **1999**, *300*, 104.

(41) Lenzer, T.; Luther, K.; Troe, J.; Gilbert, R. G.; Lim, K. F. *J. Chem. Phys.* **1995**, *103*, 626.

(42) Lenzer, T.; Luther, K. *J. Chem. Phys.* **1996**, *105*, 10944.

(43) Yoder, L. M.; Barker, J. R. *J. Phys. Chem. A* **2000**, *104*, 10184.

(44) Lenzer, T.; Luther, K. *J. Chem. Phys.* **1996**, *104*, 3391.

(45) Grogoleit, U.; Lenzer, T.; Luther, K. *Z. Phys. Chem.* **2000**, *214*, 1065.

(46) Clary, D. C.; Gilbert, R. G.; Bernshtein, V.; Oref, I. *Faraday Discuss.* **1995**, *102*, 423.

(47) Lendvay, G.; Schatz, G. C. *ACS Symp. Ser.* **1997**, *678*, 202. Lendvay, G.; Schatz, G. C. *Ber. Bunsen-Ges.* **1997**, *101*, 587. Schatz, G. C.; Lendvay, G. *J. Chem. Phys.* **1997**, *106*, 3548.

(48) Jordan, M. J. T.; Clary, D. C. *J. Chem. Phys.* **1997**, *106*, 5439.

(49) Hase, W. L.; Duchovic, R. J.; Hu, Komomicki, A.; Lim, K. F.; Lu, D.-H.; Peslherbe, G. H.; Swamy, K. N.; Vande Linde, S. R.; Varandas, A.; Wang, H.; Wolf, R. *Quantum Chem, Program Exchange Bull.* **1996**, *16*, 43 [QCPE Program 671].

(50) Brumer, P. Private communication.

(51) Humphrey, W.; Dalke, A.; Schulten, K. *J. Mol. Graphics* **1996**, *14*, 33.

(52) Hase, W. L. Private communication.

(53) Billes, F.; Billes, H.; Mikosch, S.; Holly, *J. Mol. Structure (THEOCHEM)* **1998**, *423*, 225.

(54) Billes, F. Private communication.

(55) PC−Spartan Pro, Wavefunction, Inc., 18401 VonKarnnan, Suite 370, Irvine, CA 92612.

(56) Lim, K. F. *J. Chem. Phys.* **1994**, *100*, 7385.

(57) Lim, K. F.; Gilbert, R. G. *J. Chem. Phys.* **1990**, *94*, 72.

(58) Hirschfelder, J. O.; Curtiss, C. F.; Bird, R. B. *Molecular Theory of Gases and Liquids*; Wiley: New York, 1954.